

DMD 043158

Predictions of CYP-Mediated Drug-Drug Interactions Using Cryopreserved
Human Hepatocytes: Comparison of Plasma and Protein-Free Media
Incubation Conditions

Jialin Mao, Michael A. Mohutsky, John P. Harrelson, Steven A. Wrighton and Stephen
D. Hall

Drug Disposition, Lilly Research Labs, Eli Lilly and Co., Indianapolis, IN (JM, MAM,
SAW and SDH); School of Pharmacy, Pacific University, Hillsboro, OR (JPH)

Running title: CYP2C9, CYP2D6 and CYP3A DDI Predictions Using Human Hepatocytes

To whom correspondence should be addressed:

Stephen D. Hall, Ph.D.

Drug Disposition

Lilly Research Labs, Eli Lilly and Co.

Lilly Corporate Center

Indianapolis, IN, 46285

Phone: 317-277-0338

Fax: 317-433-9287

Email: HALL_STEPHEN_D@LILLY.COM

The number of text pages: 25

The number of tables: 4

The number of figures: 3

The number of reference: 86

The number of words in the *Abstract*: 249

The number of words in the *Introduction*: 397

The number of words in the *Discussion*: 1781

Abbreviations: AUC: area under the curve; CYP3A/CYP2C9/CYP2D6: cytochrome P450 3A/2C9/2D6; DDIs: drug-drug interactions; K_m : Michaelis-Menten constant; V_{max} : maximum rate of metabolism; $f_{u,p}$: fraction unbound in human plasma; TDI: time-dependent inhibitor; HLM: human liver microsomes; HMM: hepatocyte maintenance medium; HHSHP: cryopreserved human hepatocytes suspended in human plasma

Abstract

Cryopreserved human hepatocytes suspended in human plasma (HHSHP) have previously provided accurate CYP3A drug-drug interaction (DDI) predictions from a single IC_{50} that captures both reversible and time-dependent inhibition. The goal of this study was to compare the accuracy of DDI predictions by a protein-free human hepatocyte system combined with the fraction unbound in plasma for inhibitor(s) with those obtained with protein-containing incubations. Seventeen CYP3A, CYP2C9 or CYP2D6 inhibitors were incubated with hepatocytes in human plasma or hepatocyte maintenance medium (HMM) for 20 min over a range of concentrations after which midazolam 1'-hydroxylation, diclofenac 4'-hydroxylation or (R)-bufuralol 1'-hydroxylation were used to quantify the corresponding CYP catalytic activities. Two methods were utilized to predict the human exposure ratio of the victim drug in the presence and absence of inhibitor. The HMM $K_{i, app}$ values were combined with the free average systemic plasma concentration ("*free [I] with HMM $K_{i, app}$* ") and the plasma $K_{i, app}$ values were combined with the total average systemic plasma concentration ("*total [I] with Plasma $K_{i, app}$* "). Of 63 clinical DDI studies, the "*total [I] with Plasma $K_{i, app}$* " method predicted 89% of cases within 2-fold of the reported interaction whereas the "*free [I] with HMM $K_{i, app}$* " method predicted only 59%. There was a general underprediction by the "*free [I] with HMM $K_{i, app}$* " method, which is consistent with an underestimation of *in vitro* inhibition potency in this system. In conclusion, the HHSHP system proved to be a simple, accurate predictor of DDIs for 3 major CYPs and superior to the protein-free approach.

Introduction

In studies of drug disposition, it has often been assumed that an *in vitro* drug metabolizing systems used for clearance and DDI predictions perform equally well in the presence or absence of protein. Consequently the expectation is that after correcting for drug protein binding, the intrinsic clearance and inhibition potencies obtained with or without protein should be equivalent but exceptions to this expectation have been noted. Enhanced unbound clearance of rose bengal, oleic acid, sulfobromophthalein and bilirubin in the presence of albumin, relative to the absence of albumin, led to postulates that an albumin receptor present on the hepatocellular membrane facilitated hepatic elimination or that a protein binding dissociation rate limitation existed (Forker et al., 1982; Svenson et al., 1974; Goresky and Rose, 1977; Reed, 1977; Weisiger et al., 1981). Although the unexpected effects of albumin on hepatic clearance led to complex hypotheses the reliability of the intrinsic clearance estimation in the presence and absence of protein was not investigated in these studies.

Human hepatocytes have been used in several formats to predict drug clearance *in vivo* (Houston and Carlile, 1997; Li et al., 1999; Blanchard et al., 2006; Hallifax et al., 2008) and more recently to predict DDIs (McGinnity et al., 2005; Zhao et al., 2005; Lu et al., 2007; Xu et al., 2009). Hepatocytes with a functioning cell membrane barrier and a realistic complement of phase I and phase II enzymes and their necessary coenzymes and cofactors, can be seen as better *in vitro* model for the quantitation of DDIs. However, a systematic comparison of the performance of hepatocytes DDI assays with and without human plasma has not been conducted (Lu et al., 2007; Lu et al., 2008a; Lu et al., 2008b). A previous study from this laboratory demonstrated that a method using an IC_{50} measured from a single time point in human hepatocytes suspended in human plasma (HHSHP) provided a highly reliable CYP3A-mediated DDI prediction for both reversible inhibitors and TDIs (Mao et al., 2011). Therefore, the similar approach has been expanded to CYP2C9 and CYP2D6 inhibitors. A comprehensive evaluation was undertaken to determine whether HHSHP or protein-free hepatocyte maintenance media (HMM) provide

reliable and comparable DDI predictions using four reversible and two time dependent CYP3A inhibitors (HSHSP data was obtained from our previous publication Mao et al., 2011), six reversible CYP2C9 inhibitors and six CYP2D6 inhibitors (five reversible inhibitors and one TDI).

Materials and Methods

Materials. Cryopreserved human hepatocytes (pool of five individuals) and InVitro GRO™ HT Medium were obtained from Celsis In Vitro Technologies, Inc. (Baltimore, MD). Midazolam, 1'-hydroxymidazolam, [¹³C₅]-1'-hydroxymidazolam, 4'-hydroxydiclofenac, [¹³C₆]-4'-hydroxydiclofenac, 1'-hydroxybufuralol and [²H₉]-1'-hydroxybufuralol were obtained from BD Gentest (Woburn, MA). Conivaptan was obtained from an internal Lilly chemical library. Diclofenac, diphenhydramine, duloxetine, fluconazole, fluvastatin, fluoxetine, ibuprofen, ketoconazole, nefazodone, miconazole, paroxetine, quinidine, sertraline, sulfaphenazole and tolbutamide were obtained from Sigma (St. Louis, MO). Aprepitant, (R)-bufuralol and voriconazole were obtained from Toronto Research Chemicals (North York, ON, Canada). Human plasma (Na-heparin) was obtained from Lampire Biological Laboratories, Inc. (Pipersville, PA). Hepatocyte Maintenance Medium (HMM) was obtained from Lonza, Inc. (Walkersville, MD).

Hepatocyte studies. Hepatocytes were thawed in InVitro GRO™ HT Medium (25 ml per 5 million hepatocytes) and centrifuged (50×g) at room temperature for 5 min. The cell pellet was reconstituted in HMM and cell viability was found to be at least 80% using a Vi-Cell XR cell viability analyzer (Beckman Coulter Inc., Brea, CA). After the cell viability was determined, hepatocytes were centrifuged at 50×g at room temperature for 5 min and resuspended in HMM or human plasma (1×10⁶ cells/ml for kinetic studies and 2×10⁶ cells/ml for inhibition studies). The cell suspension was incubated at 37 °C with 5% CO₂ and 95% O₂ before use. HMM is protein-free hepatocyte maintenance medium, and its content is similar to Williams' E Medium containing water, inorganic salts, amino acids and vitamins with no growth factors.

Kinetic studies. The stock hepatocyte suspension in HMM or human plasma (50 μl) was added to 50 μl of HMM or human plasma containing probe substrates such that the final concentration of hepatocytes was 0.5 × 10⁶ cells/ml. Preliminary studies were conducted to determine the substrate range necessary to achieve maximal activity for each CYP-substrate pair. For CYP3A, final

midazolam concentrations were 1.25 - 160 μM (HMM) and 15 - 1920 μM (human plasma). For CYP2C9, final diclofenac concentrations were 1.5 - 192 μM (HMM) and 75 - 9600 μM (human plasma). For CYP2D6, the final concentration range of (R)-bufuralol in both HMM and human plasma was 2.25 - 288 μM . All incubations were conducted at 37 °C and 5% CO₂. Incubations were terminated after 35, 45 and 25 minutes for CYP3A, CYP2C9, and CYP2D6, respectively by adding 200 μl of acetonitrile/methanol (3:1 v/v) containing the respective internal standard (150 nM [¹³C₅]-1'-hydroxymidazolam for CYP3A, 945 nM [¹³C₆]-4'-hydroxydiclofenac for CYP2C9, and 80 nM [²H₉]-1'-hydroxybufuralol for CYP2D6). Samples were centrifuged at 4000 rpm for 20 min and an aliquot of the supernatant was analyzed by LC-MS/MS. Preliminary experiments demonstrated that these incubation conditions resulted in linear formation of 1'-hydroxymidazolam, 4'-hydroxydiclofenac and 1'-hydroxybufuralol with respect to incubation time and hepatocyte concentration at both high and low substrate concentrations.

Inhibition studies. The studies with HHSHP and CYP3A inhibitors have appeared elsewhere (Mao et al., 2011) and are included here to allow for direct comparison to the studies with hepatocytes suspended in protein-free HMM. The same hepatocytes lot was utilized for conducting all studies presented here. CYP3A inhibitor concentrations in HMM and human plasma were 0.03 - 20 μM for ketoconazole and 0.13 - 100 μM for aprepitant, conivaptan (TDI), fluconazole, nefazodone (TDI) and voriconazole. CYP2C9 inhibitor concentrations in HMM and human plasma were 0.13 - 100 μM for fluconazole, miconazole, sulfaphenazole and fluvastatin, and 1.65 - 1200 μM for ibuprofen and tolbutamide. CYP2D6 inhibitor concentrations in HMM and human plasma were 0.13 - 100 μM for diphenhydramine, duloxetine and sertraline, 0.0013 - 1 μM for quinidine, 0.013 - 10 μM for paroxetine (TDI), and 0.03 - 20 μM for fluoxetine. The final organic vehicle concentration was 0.5% methanol. Incubations were performed in triplicate. The stock hepatocyte suspension in HMM or human plasma (25 μl) was added to 50 μl of HMM or human plasma containing inhibitor and incubated for 20 min (37 °C and 5% CO₂) before the addition of the probe substrate. Probe substrates were dissolved in 25 μl of HMM or human

plasma and final incubation concentrations were: 0.6 μM in HMM and 30 μM in human plasma (midazolam), 5 μM in HMM and 160 μM in human plasma (diclofenac), and 2 μM in HMM and 24 μM in human plasma ((R)-bufuralol). Following addition of the probe substrate the incubations were continued for 35, 45 and 25 min for CYP3A, CYP2C9, and CYP2D6, respectively. Incubations were terminated similar to the method used for kinetic studies by the addition of 200 μl of acetonitrile/methanol (3:1 v/v) containing the respective internal standard. Samples were centrifuged at 4000 rpm for 20 min and an aliquot of the supernatant was analyzed by LC-MS/MS.

Liquid chromatography/tandem mass spectrometry methods. Quantification of 1'-hydroxymidazolam, 4'-hydroxydiclofenac and 1'-hydroxybufuralol was achieved using HPLC (Shimadzu LC10) interfaced to a triple quadrupole mass spectrometer (Sciex API 4000, Applied Biosystems, Foster City, CA).

CYP3A. Detailed HPLC/MS conditions for the chromatographic separation for 1'-hydroxymidazolam were previously described (Mao et al., 2011).

CYP2C9. Chromatographic separation for 4'-hydroxydiclofenac was achieved using a reverse phase column (Varian Monochrome 5 μm C18 column, 50 \times 2 mm, Varian, Palo Alto, CA) with a gradient consisting of 5% methanol in 5 mM ammonium acetate (mobile phase A) and 95% methanol in 5 mM ammonium acetate (mobile phase B) at a flow rate of 0.5 ml/min with 5 μl injection volume. Specifically, mobile phase B (20%) was increased linearly to 99% from 0 to 1.15 min, and was held at 99% from 1.15 to 2.40 min, and the column was re-equilibrated to 20% B. The electrospray ionization probe was run in the negative mode with probe temperature of 450 $^{\circ}\text{C}$. The m/z transitions of 4'-hydroxydiclofenac and [$^{13}\text{C}_6$]- 4'-hydroxydiclofenac were 310 \rightarrow 266 and 316 \rightarrow 272, respectively. The lower and upper limits of quantification were 113 and 14418 nM 4'-hydroxydiclofenac. The interday accuracy ranged from -7.4% to -1.4%, and the intraday accuracy ranged from -10.9% to 0.9%. The interday precision ranged from 1.4% to 7.5%, and the intraday precision ranged from 1.1% to 8.2%.

CYP2D6. Chromatographic separation for 1'-hydroxybufuralol was achieved using a reverse phase column (Varian Monochrome 5 μ m C18 column, 50 \times 2 mm, Varian, Palo Alto, CA) with a gradient consisting of 5% methanol in 5 mM ammonium acetate (mobile phase A) and 95% methanol in 5 mM ammonium acetate (mobile phase B) at a flow rate of 0.5 mL/min with 5 μ l injection volume. Specifically, mobile phase B (10%) was increased linearly to 90% from 0 to 1.70 min, and increased to 98% in the next 0.01 min. Mobile phase B was held at 98% from 1.71 to 2.50 min, and the column was re-equilibrated to 10% B. The electrospray ionization probe was run in the positive mode with probe temperature of 550 $^{\circ}$ C. The m/z transitions of 1'-hydroxybufuralol and [2 H $_9$]-1'-hydroxybufuralol were 278 \rightarrow 186 and 287 \rightarrow 186, respectively. The lower and upper limits of quantification were 2.45 and 624.6 nM 1'-hydroxybufuralol. The interday accuracy ranged from -8.1% to -1.6%, and the intraday accuracy ranged from -6.8% to 6.7%. The interday precision ranged from 2.7% to 7.1%, and the intraday precision ranged from 1.2% to 4.4%.

Data analysis.

Kinetic data. Kinetic parameters (V_{\max} and K_m) for each substrate in HMM and human plasma (based on the nominal concentration, no correction of unbound fraction) were obtained by fitting the untransformed data to the Michaelis-Menten equation (Eq. 1) using weighted nonlinear regression (WinNonlin 5.0, Pharsight Corp, Mountain View, CA).

$$V = \frac{[S] \times V_{\max}}{K_m + [S]} \quad (\text{Eq.1})$$

Inhibition data. A same approach was described previously (Mao et al., 2011), in which the relationship between the CYP activities in hepatocytes incubated in both systems at a given time and inhibitor concentration relative to the baseline CYP activity was used to determine an IC_{50} . IC_{50} values were calculated with the mean of triplicate determinations using the following model (Eq. 2) by weighted nonlinear regression (WinNonlin 5.0, Pharsight Corp, Mountain View, CA).

$$Y = \frac{a}{1 + (X/IC_{50})^{\gamma}} \quad (\text{Eq.2})$$

Where X is the nominal concentration of an inhibitor (no correction of $f_{u,p}$ for the human plasma incubation); Y represents the percentage of baseline CYP activity remaining; a is the estimated response at zero concentration of inhibitor; γ is the slope factor, which describes the steepness of the curve.

The apparent $K_{i,app}$ for each inhibitor in HMM or human plasma was calculated by the following equation (Eq. 3).

$$K_{i,app} = \frac{IC_{50}}{1 + [S]/K_m} \quad (\text{Eq. 3})$$

where K_m is the Michaelis-Menten constant for 1'-hydroxymidazolam, 4'-hydroxydiclofenac and 1'-hydroxybufuralol formation obtained in either HMM or human plasma, and $[S]$ represents the concentration of midazolam, diclofenac and (R)-bufuralol in the HMM and plasma inhibition assays.

Predictions of drug-drug interactions.

CYP3A. A general model (Eq. 5) of enzyme inhibition was used to predict a potential increase in exposure to a drug as a result of the inhibition of hepatic and intestinal CYP3A (Ito et al., 1998; Wang et al., 2004; Obach et al., 2006). For competitive inhibitors, the $K_{i,app}$ would be equivalent to the inhibition constant K_i . In the case of TDIs, $K_{i,app}$ would be equivalent to $K_I \times k_{deg} / k_{inact}$ when $[I] \ll K_I$, where k_{deg} is degradation rate constant of CYP3A, K_I is the inhibitor concentration required for half maximal inactivation, and k_{inact} is the maximum inactivation rate constant (Wang et al., 2004).

$$\frac{AUC_{p.o,i}}{AUC_{p.o}} = \frac{CL_{u,int}}{CL_{u,int,i}} = \frac{1}{[f_{m,CYP3A} / (1 + [I]/K_{i,app})] + (1 - f_{m,CYP})} \times \frac{1}{[(1 - F_g) / (1 + [I]_g / K_{i,app} \times f_{u,p})] + F_g}$$

(Eq. 5)

$AUC_{p.o,i}/AUC_{p.o}$ is the predicted ratio of *in vivo* exposure of a CYP3A-cleared drug with and without oral coadministration of the inhibitor, $f_{m,CYP}$ is the fraction of total clearance CYP3A contributes for the affected drug, F_g is the fraction of the dose of the affected drug that passes through the intestine unchanged after p.o. administration in the control state. In four clinical studies (ketoconazole, aprepitant, conivaptan, and voriconazole) intravenous midazolam dosing was employed and AUC ratio was predicted using Eqs. 5 and 6 with $F_g = 1$ and under the reasonable assumption that midazolam has a low to moderate hepatic extraction ratio.

The fraction of midazolam metabolized by CYP3A was assumed to be 0.93 as observed previously (Obach et al., 2006). The fraction of drug metabolized by CYP3A in the intestine was assumed to be 1 (assuming no other CYPs other than CYP3A metabolize midazolam in the intestine), and the F_g values for midazolam, was assumed to be 0.57, as described previously (Ernest et al., 2005; Obach et al., 2006). Inhibitor concentrations were collected from three main sources. The average systemic plasma concentration of the inhibitor reported or calculated (i.e., plasma concentration area under curve from 0 to the dosing interval ($AUC_{0-\tau}$) divided by the dosing interval) from the primary literature was the preferred source. The second option utilized the inhibitor concentration at a specific time point reported in the primary literature. If the inhibitor concentration was not reported in the primary literature, values were obtained from secondary literature sources (Ito et al., 2003; Einolf, 2007; Fahmi et al., 2008; Fahmi et al., 2009). These values were previously derived from other literature in which similar dosing regimens were employed for individual inhibitors.

The concentration of the inhibitor in the enterocyte during absorption ($[I]_g$) (Eq. 6) was estimated based on the assumption that 1) no significant protein binding in the gut lumen and 2) inhibitors not subject to any first pass metabolism (Rostami-Hodjegan A, 2004; Galetin et al., 2008). D is the dose of the inhibitor (mg), k_a is the oral absorption rate constant of the inhibitor, F_a is the fraction of the inhibitor absorbed into the gut wall from the intestinal

lumen following oral administration, Q_{ent} represents the blood flow to the enterocyte, and MW is the molecule weight for each inhibitor. For k_a and Q_{ent} values of 0.03 min^{-1} and 248 ml/min were respectively used, as described previously (Obach et al., 2006). An F_a value of 1 was used for all drugs (Einolf, 2007).

$$[I]_g = \frac{D \times k_a \times F_a}{Q_{ent} \times MW} \quad (\text{Eq. 6})$$

For HMM $K_{i,app}$, the free systemic plasma concentration ($[I] \times f_{u,p}$) was employed for DDI predictions because the HMM $K_{i,app}$ was generated in a plasma protein-free environment (the “free $[I]$ with HMM $K_{i,app}$ ” method).

For plasma $K_{i,app}$, the total systemic plasma concentration was employed for hepatic DDI prediction (the “total $[I]$ with plasma $K_{i,app}$ ” method). The plasma $K_{i,app}$ values were based on total inhibitor concentration in plasma and consequently there was no need to use unbound plasma concentrations in the predictions. The prediction of intestinal inhibition, $K_{i,app}$ values were converted to unbound values ($K_{i,app} \times f_{u,p}$) consistent with the assumption of no significant plasma protein binding in the gut lumen. The fraction unbound in human plasma ($f_{u,p}$) for each compound was collected from Goodman & Gilman (Hardman et al., 2001).

CYP2C9 and CYP2D6. A similar model (Eq.7) without considering the intestinal interaction was utilized for CYP2C9 and CYP2D6 inhibition.

$$\frac{AUC_{p.o,i}}{AUC_{p.o}} = \frac{CL_{u,int}}{CL_{u,int,i}} = \frac{1}{[f_{m,CYP} / (1 + [I]/K_{i,app})] + (1 - f_{m,CYP})} \quad (\text{Eq. 7})$$

The values for the fraction of object drug metabolized by CYP2C9 were assumed to be the same as that reported previously for tolbutamide, phenytoin, S-warfarin, lovastatin, fluvastatin, glimepiride and diclofenac (0.80, 0.75, 0.87, 0.81, 0.60, 0.95 and 0.75, respectively) (Brown et al., 2005). Likewise, the values for the fraction of object drug metabolized by CYP2D6 were 0.83, 0.88, 0.46, 0.86, 0.49 and 0.76 for metoprolol, desipramine, imipramine, encainide,

mexiletine, and propafenone, respectively (Brown et al., 2005). Values of the inhibitor concentration were adopted from the calculated average systemic plasma concentration after repeated oral administration (Ito et al., 2003).

Data sources. Data from 63 clinical DDI studies were collected from the primary literature after having been identified by the University of Washington Metabolism and Transport Drug Interaction Database (<http://www.druginteractioninfo.org/>). The database was accessed on 06/24/2009, and the data are reported in Table 3.

Seventeen inhibitors were chosen based on the following considerations: 1) representative reversible inhibitors (i.e., ketoconazole a strong CYP3A inhibitor; sulfaphenazole, fluvastatin and miconazole strong CYP2C9 inhibitors; duloxetine, fluoxetine and quinidine strong CYP2D6 inhibitors; fluconazole a moderate CYP3A and CYP2C9 inhibitor, voriconazole and aprepitant moderate CYP3A inhibitors; ibuprofen and tolbutamide moderate CYP2C9 inhibitors; diphenhydramine and sertraline moderate CYP2D6 inhibitors) and TDIs (nefazodone and conivaptan moderate CYP3A TDIs; paroxetine a strong CYP2D6 TDI); 2) compounds with varied levels of plasma protein binding (conivaptan, ketoconazole, fluvastatin, miconazole, ibuprofen, tolbutamide, duloxetine, fluoxetine, paroxetine, quinidine and sertraline high plasma protein binding; voriconazole, sulfaphenazole and diphenhydramine moderate plasma protein binding; and fluconazole low plasma protein binding).

Nineteen clinical DDI studies involved the inhibition of CYP3A with midazolam as the victim drug (three studies were related to TDIs); 15 studies involved the inhibition of CYP2C9 with tolbutamide, phenytoin, S-warfarin, lovastatin, fluvastatin, glimepiride and diclofenac as victim drugs; 29 studies involved the inhibition of CYP2D6 with metoprolol, desipramine, imipramine, encainide, mexiletine, and propafenone as the victim drugs (eight studies were related to paroxetine).

Data analyses. Among 63 clinical DDIs, there were 15 strong interactions (AUC ratio > 5), 25 moderate interactions ($2 \leq \text{AUC ratio} \leq 5$), 17 weak interactions ($1.25 \leq \text{AUC ratio} < 2$) and 6 no interaction (AUC ratio < 1.25, assuming no induction). Two methods were employed to quantify the accuracy of predicted DDIs. One was to compare the fold error of the ratio of predicted to observed AUC values (2-fold cut-off). The second method was called “categorical prediction” based on the definition of strong, moderate, weak, and no interactions (Draft FDA Guidance for Industry 2006, Drug Interaction Studies-Study Design, Data Analysis, and Implications for Dosing and Labeling; <http://www.fda.gov/Drugs/DevelopmentApprovalProcess/DevelopmentResources/DrugInteractionsLabeling/ucm080499.htm>).

In addition, the bias and precision of both methods were evaluated by the geometric mean-fold error (GMFE) and the root-mean-square error (RMSE) with equations 8 and 9, respectively.

$$\text{GMFE} = 10^{\frac{\sum \left| \log\left(\frac{\text{Predicted DDI}}{\text{Observed DDI}}\right) \right|}{\text{Number of predictions}}} \quad (\text{Eq. 8})$$

$$\text{RMSE} = \sqrt{\frac{\sum (\text{Predicted DDI} - \text{Observed DDI})^2}{\text{Number of predictions}}} \quad (\text{Eq. 9})$$

Results

Substrate kinetic studies

Midazolam 1'-hydroxylation, diclofenac 4'-hydroxylation and (R)-bufuralol 1'-hydroxylation data from human hepatocytes in HMM and human plasma were fitted to the Michaelis-Menten equation. The K_m values were referenced to the nominal total concentration in the individual study system and also referenced to the corresponding unbound concentration for the plasma system; values in the HMM system were not corrected for nonspecific binding. Overall, K_m values were higher in plasma than HMM for all three CYP-substrate pairs while maximal velocities were similar in both systems. The K_m for midazolam 1'-hydroxylation in human plasma (Table 1) was approximately 6-fold higher than that in HMM (46 μM vs. 8 μM), although the maximum rates of 1'-OH midazolam formation in both systems were within 2-fold (0.036 and 0.021 nmol/min/million cells in human plasma and HMM, respectively). The K_m of diclofenac in human plasma was about 41-fold higher than that in HMM (1408 μM vs. 35 μM), while the maximum rates of 4'-OH diclofenac formation in both systems were comparable (0.49 and 0.41 nmol/min/million cells in human plasma and HMM, respectively). The K_m of (R)-bufuralol in human plasma was approximately 4.5-fold higher than that in HMM (55 μM vs. 12 μM), and the maximum rates of (R)-bufuralol metabolism in both systems were comparable (0.048 and 0.059 nmol/min/million cells in human plasma and HMM, respectively). When corrected for protein binding the plasma K_m values were generally lower than those estimated in the HMM system (Table 1).

Enzyme inhibition parameter estimation

CYP3A

Six inhibitors were incubated with human hepatocytes suspended in human plasma (Mao et al., 2011) or HMM for 20 min over a range of concentrations in the absence of midazolam and

a further 35 min in the presence of midazolam. The IC_{50} value for each inhibitor was estimated using Eq. 1 and the values are shown in Table 2. Due to solubility issues, no IC_{50} value was obtained in HMM system for aprepitant. The addition of human plasma facilitated the solubility of aprepitant and an IC_{50} curve was obtained in this system ($IC_{50} = 24.10 \mu M$). Based on the assumption that the nominal concentration of inhibitor mimics the extracellular concentration, these IC_{50} values represent the total concentration of the inhibitors that inhibit 50% of CYP3A activity. The mean IC_{50} values were converted to the corresponding $K_{i,app}$ in HMM and plasma (listed in Table 3) considering the difference in K_m values measured in each system according to Eq. 3. Assuming there is minimal nonspecific binding, the ratio of HMM $K_{i,app}$ and plasma $K_{i,app}$ are expected to be equal to $f_{u,p}$ because the plasma $K_{i,app}$ was generated using total inhibitor concentration while the HMM $K_{i,app}$ was generated using free inhibitor concentration. Therefore, in order to compare the values of $K_{i,app}$ generated from two matrices, the plasma $K_{i,app}$ corrected by $f_{u,p}$ was plotted against HMM $K_{i,app}$ in Figure 1. In order to prevent bias in the collection and use of $f_{u,p}$, the values of $f_{u,p}$ were obtained from a single source, Goodman & Gilman (Hardman et al., 2001). For all five CYP3A inhibitors, the values of HMM $K_{i,app}$ were higher than the plasma $K_{i,app}$ corrected by $f_{u,p}$.

CYP2C9

Six inhibitors were incubated with human hepatocytes suspended in human plasma or HMM for 20 min over a range of concentrations in the absence of diclofenac and a further 45 min in the presence of diclofenac. The IC_{50} value for each inhibitor was estimated using Eq. 1 and the values are shown in Table 2. For fluconazole, the plasma IC_{50} value was comparable to that previously reported (Lu et al., 2007; Lu et al., 2008a; Lu et al., 2008b). These IC_{50} values were converted to the corresponding $K_{i,app}$ in HMM and plasma (listed in Table 3) considering the difference in K_m values measured in each system according to the Eq. 3. Although plasma $IC_{50,app}$ values of ibuprofen and tolbutamide are higher than $1200 \mu M$, the plasma $K_{i,app}$ was calculated as the plasma $IC_{50,app}$ of $1200 \mu M$ in order to perform the DDI prediction. Despite this, no DDI was

predicted for ibuprofen and tolbutamide. With the exception of sulfaphenazole, the values of HMM $K_{i, app}$ were higher than the plasma $K_{i, app}$ corrected by $f_{u,p}$ (Figure 1), which was also observed with CYP3A inhibitors. Fluconazole had a higher $K_{i, app}$ value in HMM than plasma for both CYP3A and CYP2C9.

CYP2D6

Six inhibitors were incubated with human hepatocytes suspended in human plasma or HMM for 20 min over a range of concentrations in the absence of the probe substrate and a further 25 min in the presence of (R)-bufuralol. (R)-bufuralol was selected rather than racemic bufuralol because CYP2D6 displays substrate enantioselectivity for (R)-bufuralol over (S)-bufuralol (Dayer et al., 1987; Narimatsu et al., 2003; Masuda et al., 2005). CYP2D6 is responsible for 95% of racemic bufuralol 1'-hydroxylation clearance, whereas CYP2C19 is responsible for 5% and CYP1A2 has a small contribution (<1%) (Mankowski, 1999).

The IC_{50} value for each inhibitor was estimated using Eq. 1 and the values are shown in Table 2. There were no major differences in IC_{50} values in HMM and plasma for quinidine and paroxetine. All IC_{50} values were converted to the corresponding $K_{i, app}$ in HMM and plasma (listed in Table 3) considering the difference in K_m values measured in each system according to the Eq. 3. With the exception of diphenhydramine, the values of HMM $K_{i, app}$ were higher than plasma $K_{i, app}$ corrected by $f_{u,p}$ (Figure 1), which was also observed with the CYP3A and CYP2C9 inhibitors.

Prediction of DDIs

Two methods were utilized for DDI predictions with six CYP3A inhibitors, six CYP2C9 inhibitors and six CYP2D6 inhibitors in 63 clinical studies (Table 3). The assumptions behind these two methods were that for the “free [I] with HMM $K_{i, app}$ ” method, HMM $K_{i, app}$ represents the “free” inhibition potency therefore the *in vivo* inhibitor concentration needs to be corrected by $f_{u,p}$. On the other hand for the “total [I] with plasma $K_{i, app}$ ” method, plasma $K_{i, app}$ represents the “total” inhibition potency therefore there is no need to correct the *in vivo* inhibitor concentration by $f_{u,p}$. Two criteria (2-fold cut-off and “categorical prediction”) were utilized to evaluate the

prediction outcomes (refer to “Materials and Methods” section for details). The predictive performance from both methods is summarized for individual CYP and all CYPs combined in Table 4.

CYP3A

Free [I] with HMM $K_{i,app}$

Five out of nineteen studies were predicted within 2-fold (26% accuracy). This method failed to predict four out of nineteen studies (Figure 2; Table 3 and 4). The HMM system could not be used to predict four aprepitant clinical DDIs since no measurement of $K_{i,app}$ could be obtained due to the poor aprepitant solubility in HMM. In addition, this method underpredicted the other 15 clinical studies by up to 8.24-fold for the ketoconazole study reported by Olkkola et al. (1994). With respect to categorical prediction, neither of the two clinical studies were correctly predicted as weak interactions (0% accuracy), two out of nine clinical studies were correctly predicted as moderate interactions (22% accuracy), and none of the eight clinical studies were correctly predicted as strong interactions (0% accuracy).

Total [I] with plasma $K_{i,app}$

Sixteen out of nineteen studies were predicted within 2-fold (84% accuracy) including four aprepitant clinical DDIs (Figure 3; Tables 3 and 4). Two out of two clinical studies were correctly predicted as weak interactions (100% accuracy), six out of nine clinical studies were correctly predicted as moderate interactions (67% accuracy), and five out of eight clinical studies were correctly predicted as strong interactions (63% accuracy).

CYP2C9

Free [I] with HMM $K_{i,app}$

Fourteen out of fifteen studies were predicted within 2-fold (93% accuracy; Figure 2 and Tables 3 and 4). For fluvastatin, ibuprofen and tolbutamide, this method predicted all 3 clinical studies within 2-fold and correctly predicted each as no interaction (100% accuracy). Although the majority of clinical studies related to fluconazole and miconazole were predicted within 2-

fold, there was a bias towards underprediction (Fig. 2). Four out of five clinical studies were correctly predicted as weak interactions (80% accuracy), two out of six clinical studies were correctly predicted as moderate interactions (33% accuracy), and the only clinical study with a strong interaction was not correctly predicted (0% accuracy).

Total [I] with plasma $K_{i,app}$

Fourteen out of fifteen studies were predicted within 2-fold (93% accuracy; Figure 3 and Tables 3 and 4). For fluvastatin, ibuprofen and tolbutamide, this method predicted all 3 clinical studies within 2-fold and correctly predicted each as no interaction (100% accuracy). With this method the predictions for 8 studies with fluconazole did not demonstrate a bias. An accurate DDI prediction for sulfaphenazole was also observed. Because of the high average plasma concentration of sulfaphenazole (160-640 μM), the maximum inhibition was reached even though the plasma $K_{i,app}$ was high. Four out of five clinical studies were correctly predicted as weak interactions (80% accuracy), four out of six clinical studies were correctly predicted as moderate interactions (66% accuracy), and the only clinical study with a strong interaction was not correctly predicted (0% accuracy).

CYP2D6

Free [I] with HMM $K_{i,app}$

Eighteen out of twenty nine studies were predicted within 2-fold (62% accuracy; Figure 2 and Tables 3 and 4). Similar to the observations with CYP3A and CYP2C9, this method underpredicted the majority of clinical DDI studies with a maximum 6.55-fold underprediction for the paroxetine study reported by Hemeryck et al. (2000). Three of three clinical studies were correctly predicted as no interactions (100% accuracy), two out of ten clinical studies were correctly predicted as weak interactions (20% accuracy; the rest were underpredicted as no interactions), one out of ten clinical studies was correctly predicted as a moderate interaction (10% accuracy), and none of six clinical studies were correctly predicted as a strong interaction (0% accuracy).

Total [I] with plasma $K_{i,app}$

Twenty six out of twenty nine studies were predicted within 2-fold (90% accuracy; Figure 3 and Tables 3 and 4). Three of three clinical studies were correctly predicted as no interactions (100% accuracy), four out of ten clinical studies were correctly predicted as weak interactions (40% accuracy; the rest were underpredicted as no interaction). Six out of ten clinical studies were correctly predicted as moderate interactions (60% accuracy), and two out of six clinical studies were correctly predicted as strong interactions (33% accuracy).

All CYPs

Free [I] with HMM $K_{i,app}$

Thirty seven out of sixty three clinical DDIs (59% accuracy) were predicted within 2-fold, and the accuracy in predicting no, weak, moderate and strong interactions was 100%, 35%, 20% and 0%, respectively (Table 4). The values of GMFE and RMSE were 0.51 and 3.94, respectively.

Total [I] with plasma $K_{i,app}$

Fifty six out of sixty three clinical DDIs (89% accuracy) were predicted within 2-fold, and the accuracy in predicting no, weak, moderate and strong interactions was 100%, 59%, 64% and 47%, respectively (Table 4). The values of GMFE and RMSE were 0.86 and 2.61, respectively.

Discussion

To evaluate the relative utility of the “total [I] with Plasma $K_{i,app}$ ” and “free [I] with HMM $K_{i,app}$ ” methods for predicting *in vivo* DDIs with cryopreserved human hepatocytes, the apparent inhibition constants were determined from protein containing and protein-free systems, respectively. After correcting for protein binding, the $K_{i,app}$ values were generally higher in the protein-free hepatocyte system, with cases showing approximately 10 to 100-fold variation (Figure 1). These system differences result in most inhibitors appearing to be more potent in the protein containing system. One explanation for this observation is that the system is modified by the presence of protein such that an enhancement of unbound intracellular inhibitor concentration occurs. This proposition would be analogous to previous discussions that question the free drug hypothesis by postulating the existence of hepatocyte membrane “albumin receptors” or an albumin-inhibitor complex “dissociation rate limited” uptake proposed for the hepatic clearance of iopanoic acid, rose bengal, sulfobromophthalein, oleate, bilirubin and palmitate (Wilkinson, 1987). The main assumption behind the “free drug” theory in the context of clearance is that the hepatic uptake of drug is solely dependent on the unbound concentration available at the surface of the liver cell, and the binding equilibrium existing within the sinusoid is maintained by the spontaneous dissociation of the protein-drug complex. However, apparent saturation kinetics were observed when the albumin-oleate complex concentration was increased at a constant fraction unbound (molar ratio of oleate to albumin constant at 1:1) in isolated perfused rat livers (Weisiger et al., 1981). This suggests that the uptake of highly protein bound compounds, such as oleate, may be attributable to an “albumin receptor” on the liver cell surface but this theory remains highly controversial despite many attempts to identify the molecular basis for such a phenomenon (Burczynski et al., 1989; Tang et al., 2002; Cui and Walter, 2003). An alternative explanation to the albumin receptor suggested that uptake removes the unbound moiety more rapidly than it can be replenished by spontaneous dissociation from albumin (see Wilkinson, 1987

for review). In this hypothesis, uptake is rate limited by dissociation from albumin and becomes proportional to the concentration of bound drug for a rapidly cleared compound (Ockner et al., 1983). More recently Iwatsubo et al., reported that the rate of hepatic uptake of compounds highly bound to albumin did not necessarily depend on the extracellular free concentration (Iwatsubo et al., 1996).

However, greater unbound inhibitor potency and unbound substrate affinity observed here in the protein containing system can be explained without dismissing the free drug hypothesis but rather by hypothesizing that there is an artefactually low intracellular inhibitor concentration in the protein-free system due to nonspecific loss of inhibitor from the extracellular environment. Although extracellular inhibitor concentrations were not measured in the current report, others have shown that substantial binding to system components can occur in non-protein media, such as the adsorption of compounds to plastic plates (DeWitte, 2006; Palmgren et al., 2006). This phenomenon can also explain why the HMM $K_{i, app}$ of fluconazole and voriconazole were higher than the corresponding plasma $K_{i, app}$ before being corrected by $f_{u,p}$. This explanation is attractive for the observations reported here not only because it is simple and preceded but also the *in vivo* DDIs examined were best predicted from the protein containing system which can be reasonably expected to be free from the nonspecific loss of inhibitor.

The higher values of HMM $K_{i, app}$ versus plasma $K_{i, app} \times f_{u,p}$ and the less accurate prediction from HMM $K_{i, app}$ suggested that the “free” inhibition potency represented by HMM $K_{i, app}$ has underpredicted the *in vivo* inhibition potency. However this does not mean that it could not serve as an *in vitro* system to measure CYP inhibition assays. Either measuring the unbound fraction of inhibitor with human hepatocytes in the protein-free incubation (equivalent medium to HMM) to correct for the nonspecific binding (McGinnity et al., 2005; Zhao et al., 2005) or incorporating the inhibitor loss to correct the inhibition potency (Zhao et al., 2005) have been employed when cryopreserved hepatocytes were utilized to generate the inhibition potency. However, both studies suggested that the improvement in DDI prediction after additional

correction steps was limited to one or two compounds, and no general recommendation for the protein-free medium was given despite the rational basis for such corrections. It is also possible that the hepatocytes maintain key metabolic capabilities in the presence of plasma and consequently provide better DDI predictions.

McGinnity et al. compared the IC_{50} values of 14 drugs obtained between cDNA expressed CYP2C9 (rCYP2C9) and cryopreserved human hepatocytes in hepatocyte suspension buffer (similar to HMM) (McGinnity et al., 2005). The CYP2C9 $IC_{50, \text{apparent}}$ values generated in human hepatocytes were systematically higher than those determined with rCYP2C9, and there was a correlation between $IC_{50, \text{unbound}}$ values generated in the different milieu after correcting for nonspecific binding. It is interesting to note that the unbound fractions of 14 drugs in hepatocytes suspension buffer are lower than that of recombinant enzyme, which suggests that there is more nonspecific binding in hepatocytes suspension buffer for CYP2C9 inhibitors. However, the method employed by these investigators significantly under predicted the majority of the DDIs examined.

Zhao and colleagues compared the IC_{50} values of six CYP3A inhibitors measured in cryopreserved human hepatocytes (suspended in William's E Medium) to that predicted with human liver microsomes (HLM), although there was no attempt to predict DDIs from the *in vitro* parameters (Zhao et al., 2005). Hepatocyte IC_{50} values were 2- to 60-fold higher than those measured in HLMs after correcting for factors such as nonspecific binding and inhibitor consumption in hepatocytes. In addition, the reported hepatocyte IC_{50} values for diltiazem, erythromycin and troleandomycin from Zhao's investigation (3.22, 18.02 and 2.14 μM , respectively) were higher than plasma $IC_{50, \text{app}}$ (2.28, 2.58, 0.23 μM , respectively) from incubations with hepatocytes in plasma as reported in a previous investigation from this laboratory (Mao et al., 2011). As a result, it is reasonable to speculate that if the hepatocyte IC_{50} values from Zhao's study were combined with the free inhibitor concentration utilized in the current studies, an under prediction would be expected. This example suggests that the correction

for nonspecific binding and inhibitor depletion in the HMM equivalent system may not be sufficient to result in robust DDI predictions. More recently, the hepatic clearance of twenty six compounds encompassing a 50-fold range of clearance and a wide range of protein binding was assessed with cryopreserved human hepatocytes in the presence and absence of human serum, and more accurate predictions of *in vivo* clearance were observed in the presence of the human serum (Blanchard et al., 2006).

For the purpose of predicting *in vivo* DDIs with human cryopreserved hepatocytes, the “total [I] with Plasma $K_{i,app}$ ” is superior to the “free [I] with HMM $K_{i,app}$ ” method under the conditions employed. For nineteen clinical CYP3A mediated DDIs, the “total [I] with Plasma $K_{i,app}$ ” method demonstrated a greater accuracy in predicting the observed *in vivo* DDIs (Table 3 and 4). More clinical DDIs were predicted within 2-fold of the observed DDI magnitude by the “total [I] with Plasma $K_{i,app}$ ” method, and more accurate categorical prediction of weak, moderate and strong interactions were observed. Due to the limited solubility of the CYP3A inhibitor aprepitant in HMM, no IC_{50} value was obtained. In the plasma system, however, an IC_{50} value was obtained for this poorly soluble compound and an accurate prediction was made for two weak and two moderate interactions precipitated by aprepitant. The “total [I] with plasma $K_{i,app}$ ” method was also the most predictive method relative to the “free [I] with HMM $K_{i,app}$ ” method for the twenty nine clinical CYP2D6 DDIs (Table 3 and 4). More clinical DDIs were predicted within 2-fold of the observed DDI magnitude by the “total [I] with plasma $K_{i,app}$ ” method (89% accuracy), and more accurate categorical prediction of no, weak, moderate and strong interactions were observed. However, the majority of weak interactions related to diphenhydramine and sertraline were under predicted as “no interactions” by both methods. These observations may be explained by the “substrate-dependent inhibition” phenomenon (Vandenbrink et al., 2011) whereby the *in vitro* victim-inhibitor pairs (R)-bufuralol- diphenhydramine and (R)-bufuralol-sertraline may not fully reflect the *in vivo* interaction of the clinical victim-inhibitor pairs metoprolol-diphenhydramine and desipramine/imipramine-sertraline.

The “*total [I] with plasma $K_{i,app}$* ” method was clearly superior to the “*free [I] with HMM $K_{i,app}$* ” method for predicting DDIs with CYP3A and CYP2D6 inhibitors. However, the difference in methods was much less apparent for CYP2C9 inhibitors because of the high inhibitor concentrations achieved in the sulfaphenazole clinical studies (insensitive to the difference K_i estimates) and the weak inhibition by fluconazole that is captured by both hepatocyte systems. Previous studies with HLMs failed to predict CYP2C9 mediated DDIs (Andersson et al., 2004). In contrast, the “*total [I] with plasma $K_{i,app}$* ” method accurately predicted no inhibition by fluvastatin, ibuprofen and tolbutamide (the observed and predicted AUC change in diclofenac were 1.07 and 1.12, 0.99 and 1.08, 0.93 and 1.11, respectively). Although with the HHSHP did not yield an accurate measurement of $K_{i,app}$ for ibuprofen and tolbutamide (plasma $IC_{50, app} > 1200 \mu M$), the maximum prediction (assuming $IC_{50, app} = 1200 \mu M$) predicted the interaction as 1.08 and 1.11. Therefore, the true interactions should be weaker than predicted, and this speculation was confirmed with the observed data (0.99 and 0.93, respectively).

A possible concern with this method is that there is no correction for the possible depletion of the inhibitor concentration in HHSHP. However, based on the kinetic data for midazolam, an efficiently metabolized CYP3A substrate, it is unlikely that inhibitor depletion would be a significant concern. Specifically, the media concentration of 1'-hydroxymidazolam was at most 0.7% of midazolam after the 35-minute incubation with various concentrations of the parent drug in HHSHP. Assuming 90% of midazolam is eliminated by 1'-hydroxylation and half of the 1'-hydroxymidazolam generated is further metabolized, it is estimated that 1.3% of the parent drug would be depleted during the 35-minute incubation. This would not significantly impact the assumed substrate nominal concentration of midazolam. For time dependent inhibitors the progressive loss of enzyme throughout the incubations would also serve to minimize the loss of inhibitor from the media. The molar concentration of CYP form is small compared to the total drug concentration and relatively little loss of inhibitor from the plasma can completely inhibit the entire target CYP.

In conclusion, the single time point HHSHP $K_{i,app}$ provided relatively simple and accurate DDI predictions mediated by three major drug metabolizing CYPs for both TDI and reversible inhibitors. This method simplified the prediction process by utilizing the total average systemic plasma concentration as a universal concentration for inhibitors and by obviating the need to correct for the unbound fraction in human plasma.

Acknowledgements

The authors would like to thank to Jeffrey M. Weber and Shane M. Lowery for bioanalytical support.

Authorship Contribution

Participated in research design: Mao, Mohutsky, Harrelson, Wrighton and Hall

Conducted experiments: Mao, Mohutsky and Harrelson

Performed data analysis: Mao, Mohutsky and Harrelson

Wrote or contributed to the writing of the manuscript: Mao, Mohutsky, Harrelson,
Wrighton and Hall

References

- Albers LJ, Reist C, Helmeste D, Vu R and Tang SW (1996) Paroxetine shifts imipramine metabolism. *Psychiatry Res* **59**:189-196.
- Alderman J, Preskorn SH, Greenblatt DJ, Harrison W, Penenberg D, Allison J and Chung M (1997) Desipramine pharmacokinetics when coadministered with paroxetine or sertraline in extensive metabolizers. *J Clin Psychopharmacol* **17**:284-291.
- Andersson TB, Bredberg E, Ericsson H and Sjoberg H (2004) An evaluation of the in vitro metabolism data for predicting the clearance and drug-drug interaction potential of CYP2C9 substrates. *Drug Metab Dispos* **32**:715-721.
- Ayesh R, Dawling S, Hayler A, Oates NS, Cholerton S, Widdop B, Idle JR and Smith RL (1991) Comparative effects of the diastereoisomers, quinine and quinidine in producing phenocopy debrisoquine poor metabolisers (PMs) in healthy volunteers. *Chirality* **3**:14-18.
- Back DJ, Tjia J, Monig H, Ohnhaus EE and Park BK (1988) Selective inhibition of drug oxidation after simultaneous administration of two probe drugs, antipyrine and tolbutamide. *Eur J Clin Pharmacol* **34**:157-163.
- Bergstrom RF, Peyton AL and Lemberger L (1992) Quantification and mechanism of the fluoxetine and tricyclic antidepressant interaction. *Clin Pharmacol Ther* **51**:239-248.
- Black DJ, Kunze KL, Wienkers LC, Gidal BE, Seaton TL, McDonnell ND, Evans JS, Bauwens JE and Trager WF (1996) Warfarin-fluconazole. II. A metabolically based drug interaction: in vivo studies. *Drug Metab Dispos* **24**:422-428.
- Blanchard N, Hewitt NJ, Silber P, Jones H, Coassolo P and Lave T (2006) Prediction of hepatic clearance using cryopreserved human hepatocytes: a comparison of serum and serum-free incubations. *J Pharm Pharmacol* **58**:633-641.
- Blum RA, Wilton JH, Hilligoss DM, Gardner MJ, Henry EB, Harrison NJ and Schentag JJ (1991) Effect of fluconazole on the disposition of phenytoin. *Clin Pharmacol Ther* **49**:420-425.
- Brosen K and Gram LF (1989) Quinidine inhibits the 2-hydroxylation of imipramine and desipramine but not the demethylation of imipramine. *Eur J Clin Pharmacol* **37**:155-160.
- Brosen K, Hansen JG, Nielsen KK, Sindrup SH and Gram LF (1993) Inhibition by paroxetine of desipramine metabolism in extensive but not in poor metabolizers of sparteine. *Eur J Clin Pharmacol* **44**:349-355.
- Brown HS, Ito K, Galetin A and Houston JB (2005) Prediction of in vivo drug-drug interactions from in vitro data: impact of incorporating parallel pathways of drug elimination and inhibitor absorption rate constant. *Br J Clin Pharmacol* **60**:508-518.
- Burczynski FJ, Cai ZS, Moran JB and Forker EL (1989) Palmitate uptake by cultured hepatocytes: albumin binding and stagnant layer phenomena. *Am J Physiol* **257**:G584-593.
- Chung E, Nafziger AN, Kazierad DJ and Bertino JS, Jr. (2006) Comparison of midazolam and simvastatin as cytochrome P450 3A probes. *Clin Pharmacol Ther* **79**:350-361.

- Cui Y and Walter B (2003) Influence of albumin binding on the substrate transport mediated by human hepatocyte transporters OATP2 and OATP8. *J Gastroenterol* **38**:60-68.
- Dayer P, Kronbach T, Eichelbaum M and Meyer UA (1987) Enzymatic basis of the debrisoquine/sparteine-type genetic polymorphism of drug oxidation. Characterization of bufuralol 1'-hydroxylation in liver microsomes of in vivo phenotyped carriers of the genetic deficiency. *Biochem Pharmacol* **36**:4145-4152.
- DeWitte RS (2006) Avoiding physicochemical artefacts in early ADME-Tox experiments. *Drug Discov Today* **11**:855-859.
- Eap CB, Buclin T, Cucchia G, Zullino D, Hustert E, Bleiber G, Golay KP, Aubert AC, Baumann P, Telenti A and Kerb R (2004) Oral administration of a low dose of midazolam (75 microg) as an in vivo probe for CYP3A activity. *Eur J Clin Pharmacol* **60**:237-246.
- Einolf HJ (2007) Comparison of different approaches to predict metabolic drug-drug interactions. *Xenobiotica* **37**:1257-1294.
- Ernest CS, 2nd, Hall SD and Jones DR (2005) Mechanism-based inactivation of CYP3A by HIV protease inhibitors. *J Pharmacol Exp Ther* **312**:583-591.
- Fahmi OA, Hurst S, Plowchalk D, Cook J, Guo F, Youdim K, Dickins M, Phipps A, Darekar A, Hyland R and Obach RS (2009) Comparison of different algorithms for predicting clinical drug-drug interactions, based on the use of CYP3A4 in vitro data: predictions of compounds as precipitants of interaction. *Drug Metab Dispos* **37**:1658-1666.
- Fahmi OA, Maurer TS, Kish M, Cardenas E, Boldt S and Nettleton D (2008) A combined model for predicting CYP3A4 clinical net drug-drug interaction based on CYP3A4 inhibition, inactivation, and induction determined in vitro. *Drug Metab Dispos* **36**:1698-1708.
- Forker EL, Luxon BA, Snell M and Shurmantine WO (1982) Effect of albumin binding on the hepatic transport of rose bengal: surface-mediated dissociation of limited capacity. *J Pharmacol Exp Ther* **223**:342-347.
- Funck-Brentano C, Kroemer HK, Pavlou H, Woosley RL and Roden DM (1989a) Genetically-determined interaction between propafenone and low dose quinidine: role of active metabolites in modulating net drug effect. *Br J Clin Pharmacol* **27**:435-444.
- Funck-Brentano C, Turgeon J, Woosley RL and Roden DM (1989b) Effect of low dose quinidine on encainide pharmacokinetics and pharmacodynamics. Influence of genetic polymorphism. *J Pharmacol Exp Ther* **249**:134-142.
- Galetin A, Gertz M and Houston JB (2008) Potential role of intestinal first-pass metabolism in the prediction of drug-drug interactions. *Expert Opin Drug Metab Toxicol* **4**:909-922.
- Goresky CA and Rose CP (1977) Blood-tissue exchange in liver and heart: the influence of heterogeneity of capillary transit times. *Fed Proc* **36**:2629-2634.
- Hallifax D, Galetin A and Houston JB (2008) Prediction of metabolic clearance using fresh human hepatocytes: comparison with cryopreserved hepatocytes and hepatic microsomes for five benzodiazepines. *Xenobiotica* **38**:353-367.
- Hamelin BA, Bouayad A, Methot J, Jobin J, Desgagnes P, Poirier P, Allaire J, Dumesnil J and Turgeon J (2000) Significant interaction between the nonprescription

- antihistamine diphenhydramine and the CYP2D6 substrate metoprolol in healthy men with high or low CYP2D6 activity. *Clin Pharmacol Ther* **67**:466-477.
- Hansen JM, Kampmann JP, Siersbaek-Nielsen K, Lumholtz IB, Arroe M, Abildgaard U and Skovsted L (1979) The effect of different sulfonamides on phenytoin metabolism in man. *Acta Med Scand Suppl* **624**:106-110.
- Hardman JG, Limbird LE and Gilman AG (2001) Goodman & Gilman's The Pharmacological Basis of Therapeutics, 10th ed. *McGraw-Hill New York*.
- Hemeryck A, Lefebvre RA, De Vriendt C and Belpaire FM (2000) Paroxetine affects metoprolol pharmacokinetics and pharmacodynamics in healthy volunteers. *Clin Pharmacol Ther* **67**:283-291.
- Houston JB and Carlile DJ (1997) Prediction of hepatic clearance from microsomes, hepatocytes, and liver slices. *Drug Metab Rev* **29**:891-922.
- Ito K, Brown HS and Houston JB (2003) Database analyses for the prediction of in vivo drug-drug interactions from in vitro data. *Br J Clin Pharmacol* **57**:13.
- Ito K, Iwatsubo T, Kanamitsu S, Ueda K, Suzuki H and Sugiyama Y (1998) Prediction of pharmacokinetic alterations caused by drug-drug interactions: metabolic interaction in the liver. *Pharmacol Rev* **50**:387-412.
- Iwatsubo T, Hirota N, Ooie T, Suzuki H and Sugiyama Y (1996) Prediction of in vivo drug disposition from in vitro data based on physiological pharmacokinetics. *Biopharm Drug Dispos* **17**:273-310.
- Johnson JA and Burlew BS (1996) Metoprolol metabolism via cytochrome P4502D6 in ethnic populations. *Drug Metab Dispos* **24**:350-355.
- Kantola T, Backman JT, Niemi M, Kivisto KT and Neuvonen PJ (2000) Effect of fluconazole on plasma fluvastatin and pravastatin concentrations. *Eur J Clin Pharmacol* **56**:225-229.
- Kaukonen KM, Olkkola KT and Neuvonen PJ (1998) Fluconazole but not itraconazole decreases the metabolism of losartan to E-3174. *Eur J Clin Pharmacol* **53**:445-449.
- Kazierad DJ, Martin DE, Blum RA, Tenero DM, Ilson B, Boike SC, Etheredge R and Jorkasky DK (1997) Effect of fluconazole on the pharmacokinetics of eprosartan and losartan in healthy male volunteers. *Clin Pharmacol Ther* **62**:417-425.
- Kharasch ED, Walker A, Hoffer C and Sheffels P (2005) Sensitivity of intravenous and oral alfentanil and pupillary miosis as minimally invasive and noninvasive probes for hepatic and first-pass CYP3A activity. *J Clin Pharmacol* **45**:1187-1197.
- Kurtz DL, Bergstrom RF, Goldberg MJ and Cerimele BJ (1997) The effect of sertraline on the pharmacokinetics of desipramine and imipramine. *Clin Pharmacol Ther* **62**:145-156.
- Laine K, De Bruyn S, Bjorklund H, Rouru J, Hanninen J, Scheinin H and Anttila M (2004) Effect of the novel anxiolytic drug deramciclone on cytochrome P(450) 2D6 activity as measured by desipramine pharmacokinetics. *Eur J Clin Pharmacol* **59**:893-898.
- Lam YW, Alfaro CL, Ereshefsky L and Miller M (2003) Pharmacokinetic and pharmacodynamic interactions of oral midazolam with ketoconazole, fluoxetine, fluvoxamine, and nefazodone. *J Clin Pharmacol* **43**:1274-1282.
- Lazar JD and Wilner KD (1990) Drug interactions with fluconazole. *Rev Infect Dis* **12 Suppl 3**:S327-333.

- Li AP, Lu C, Brent JA, Pham C, Fackett A, Ruegg CE and Silber PM (1999) Cryopreserved human hepatocytes: characterization of drug-metabolizing enzyme activities and applications in higher throughput screening assays for hepatotoxicity, metabolic stability, and drug-drug interaction potential. *Chem Biol Interact* **121**:17-35.
- Lu C, Berg C, Prakash SR, Lee FW and Balani SK (2008a) Prediction of pharmacokinetic drug-drug interactions using human hepatocyte suspension in plasma and cytochrome P450 phenotypic data. III. In vitro-in vivo correlation with fluconazole. *Drug Metab Dispos* **36**:1261-1266.
- Lu C, Hatsis P, Berg C, Lee FW and Balani SK (2008b) Prediction of pharmacokinetic drug-drug interactions using human hepatocyte suspension in plasma and cytochrome P450 phenotypic data. II. In vitro-in vivo correlation with ketoconazole. *Drug Metab Dispos* **36**:1255-1260.
- Lu C, Miwa GT, Prakash SR, Gan LS and Balani SK (2007) A novel model for the prediction of drug-drug interactions in humans based on in vitro cytochrome p450 phenotypic data. *Drug Metab Dispos* **35**:79-85.
- Majumdar AK, McCrean JB, Panebianco DL, Hesney M, Dru J, Constanzer M, Goldberg MR, Murphy G, Gottesdiener KM, Lines CR, Petty KJ and Blum RA (2003) Effects of aprepitant on cytochrome P450 3A4 activity using midazolam as a probe. *Clin Pharmacol Ther* **74**:150-156.
- Majumdar AK, Yan KX, Selverian DV, Barlas S, Constanzer M, Dru J, McCrean JB, Ahmed T, Frick GS, Kraft WK, Petty KJ and Greenberg HE (2007) Effect of aprepitant on the pharmacokinetics of intravenous midazolam. *J Clin Pharmacol* **47**:744-750.
- Mankowski DC (1999) The role of CYP2C19 in the metabolism of (+/-) bufuralol, the prototypic substrate of CYP2D6. *Drug Metab Dispos* **27**:1024-1028.
- Mao J, Mohutsky MA, Harrelson JP, Wrighton SA and Hall SD (2011) Prediction of CYP3A-mediated drug-drug interactions using human hepatocytes suspended in human plasma. *Drug Metab Dispos* **39**:591-602.
- Masuda K, Tamagake K, Okuda Y, Torigoe F, Tsuzuki D, Isobe T, Hichiya H, Hanioka N, Yamamoto S and Narimatsu S (2005) Change in enantioselectivity in bufuralol 1"-hydroxylation by the substitution of phenylalanine-120 by alanine in cytochrome P450 2D6. *Chirality* **17**:37-43.
- McCrean J, Prueksaritanont T, Gertz BJ, Carides A, Gillen L, Antonello S, Brucker MJ, Miller-Stein C, Osborne B and Waldman S (1999) Concurrent administration of the erythromycin breath test (EBT) and oral midazolam as in vivo probes for CYP3A activity. *J Clin Pharmacol* **39**:1212-1220.
- McGinnity DF, Tucker J, Trigg S and Riley RJ (2005) Prediction of CYP2C9-mediated drug-drug interactions: a comparison using data from recombinant enzymes and human hepatocytes. *Drug Metab Dispos* **33**:1700-1707.
- Narimatsu S, Takemi C, Kuramoto S, Tsuzuki D, Hichiya H, Tamagake K and Yamamoto S (2003) Stereoselectivity in the oxidation of bufuralol, a chiral substrate, by human cytochrome P450s. *Chirality* **15**:333-339.
- Niemi M, Backman JT, Neuvonen M, Laitila J, Neuvonen PJ and Kivisto KT (2001) Effects of fluconazole and fluvoxamine on the pharmacokinetics and pharmacodynamics of glimepiride. *Clin Pharmacol Ther* **69**:194-200.

- NDA 021697.
http://www.accessdata.fda.gov/drugsatfda_docs/nda/2005/021697s000_VaprisolT_OC.cfm
- O'Reilly RA, Goulart DA, Kunze KL, Neal J, Gibaldi M, Eddy AC and Trager WF (1992) Mechanisms of the stereoselective interaction between miconazole and racemic warfarin in human subjects. *Clin Pharmacol Ther* **51**:656-667.
- Obach RS, Walsky RL, Venkatakrishnan K, Gaman EA, Houston JB and Tremaine LM (2006) The utility of in vitro cytochrome P450 inhibition data in the prediction of drug-drug interactions. *J Pharmacol Exp Ther* **316**:336-348.
- Ockner RK, Weisiger RA and Gollan JL (1983) Hepatic uptake of albumin-bound substances: albumin receptor concept. *Am J Physiol* **245**:G13-18.
- Olkkola KT, Ahonen J and Neuvonen PJ (1996) The effects of the systemic antimycotics, itraconazole and fluconazole, on the pharmacokinetics and pharmacodynamics of intravenous and oral midazolam. *Anesth Analg* **82**:511-516.
- Olkkola KT, Backman JT and Neuvonen PJ (1994) Midazolam should be avoided in patients receiving the systemic antimycotics ketoconazole or itraconazole. *Clin Pharmacol Ther* **55**:481-485.
- Palmgren JJ, Monkkonen J, Korjamo T, Hassinen A and Auriola S (2006) Drug adsorption to plastic containers and retention of drugs in cultured cells under in vitro conditions. *Eur J Pharm Biopharm* **64**:369-378.
- Preskorn SH, Alderman J, Chung M, Harrison W, Messig M and Harris S (1994) Pharmacokinetics of desipramine coadministered with sertraline or fluoxetine. *J Clin Psychopharmacol* **14**:90-98.
- Reed RG (1977) Kinetics of bilirubin binding to bovine serum albumin and the effects of palmitate. *J Biol Chem* **252**:7483-7487.
- Rostami-Hodjegan A TG (2004) 'in Silico' simulations to assess the 'in vivo' consequences of 'in vitro' metabolic drug-drug interactions. *Drug Discovery Today* **1**:441-448.
- Saari TI, Laine K, Leino K, Valtonen M, Neuvonen PJ and Olkkola KT (2006) Effect of voriconazole on the pharmacokinetics and pharmacodynamics of intravenous and oral midazolam. *Clin Pharmacol Ther* **79**:362-370.
- Sharma A, Pibarot P, Pilote S, Dumesnil JG, Arsenault M, Belanger PM, Meibohm B and Hamelin BA (2005) Modulation of metoprolol pharmacokinetics and hemodynamics by diphenhydramine coadministration during exercise testing in healthy premenopausal women. *J Pharmacol Exp Ther* **313**:1172-1181.
- Skinner MH, Kuan HY, Pan A, Sathirakul K, Knadler MP, Gonzales CR, Yeo KP, Reddy S, Lim M, Ayan-Oshodi M and Wise SD (2003) Duloxetine is both an inhibitor and a substrate of cytochrome P4502D6 in healthy volunteers. *Clin Pharmacol Ther* **73**:170-177.
- Svenson A, Holmer E and Andersson LO (1974) A new method for the measurement of dissociation rates for complexes between small ligands and proteins as applied to the palmitate and bilirubin complexes with serum albumin. *Biochim Biophys Acta* **342**:54-59.
- Tang C, Lin Y, Rodrigues AD and Lin JH (2002) Effect of albumin on phenytoin and tolbutamide metabolism in human liver microsomes: an impact more than protein binding. *Drug Metab Dispos* **30**:648-654.

- Touchette MA, Chandrasekar PH, Milad MA and Edwards DJ (1992) Contrasting effects of fluconazole and ketoconazole on phenytoin and testosterone disposition in man. *Br J Clin Pharmacol* **34**:75-78.
- Tsunoda SM, Velez RL, von Moltke LL and Greenblatt DJ (1999) Differentiation of intestinal and hepatic cytochrome P450 3A activity with use of midazolam as an in vivo probe: effect of ketoconazole. *Clin Pharmacol Ther* **66**:461-471.
- Turgeon J, Fiset C, Giguere R, Gilbert M, Moerike K, Rouleau JR, Kroemer HK, Eichelbaum M, Grech-Belanger O and Belanger PM (1991) Influence of debrisoquine phenotype and of quinidine on mexiletine disposition in man. *J Pharmacol Exp Ther* **259**:789-798.
- Turgeon J, Pavlou HN, Wong W, Funck-Brentano C and Roden DM (1990) Genetically determined steady-state interaction between encainide and quinidine in patients with arrhythmias. *J Pharmacol Exp Ther* **255**:642-649.
- Vandenbrink BM, Foti RS, Rock DA, Wienkers LC and Wahlstrom JL (2011) Prediction of CYP2D6 Drug Interactions from In Vitro Data: Evidence for Substrate-Dependent Inhibition. *Drug Metab Dispos*.
- Venkatakrishnan K and Obach RS (2007) Drug-drug interactions via mechanism-based cytochrome P450 inactivation: points to consider for risk assessment from in vitro data and clinical pharmacologic evaluation. *Curr Drug Metab* **8**:449-462.
- Veronese ME, Miners JO, Randles D, Gregov D and Birkett DJ (1990) Validation of the tolbutamide metabolic ratio for population screening with use of sulfaphenazole to produce model phenotypic poor metabolizers. *Clin Pharmacol Ther* **47**:403-411.
- Wang YH, Jones DR and Hall SD (2004) Prediction of cytochrome P450 3A inhibition by verapamil enantiomers and their metabolites. *Drug Metab Dispos* **32**:259-266.
- Weisiger R, Gollan J and Ockner R (1981) Receptor for albumin on the liver cell surface may mediate uptake of fatty acids and other albumin-bound substances. *Science* **211**:1048-1051.
- Wilkinson GR (1987) Clearance approaches in pharmacology. *Pharmacol Rev* **39**:1-47.
- Xu L, Chen Y, Pan Y, Skiles GL and Shou M (2009) Prediction of human drug-drug interactions from time-dependent inactivation of CYP3A4 in primary hepatocytes using a population-based simulator. *Drug Metab Dispos* **37**:2330-2339.
- Zhao P, Kunze KL and Lee CA (2005) Evaluation of time-dependent inactivation of CYP3A in cryopreserved human hepatocytes. *Drug Metab Dispos* **33**:853-861.
- Zussman BD, Davie CC and Fowles SE (1995) Sertraline, like other SSRIs, is a significant inhibitor of desipramine metabolism in vivo. *Br J Clin Pharmacol*. **39**:1.

Footnotes

Current address for JM: Department of Drug Metabolism and Pharmacokinetics,
Genentech, A Member of the Roche Group; SAW: W925 Miramar Dr, East Troy, WI
53120

Figure Legends

Figure 1. Comparison of HMM $K_{i,app}$ and plasma $K_{i,app} \times f_{u,p}$. The solid line depicts the line of unity. Values of HMM $K_{i,app}$ and plasma $K_{i,app}$ are listed in Table 3, which were calculated from measured HMM and plasma $IC_{50,app}$. Unbound fraction ($f_{u,p}$) were collected from Goodman & Gilman's The Pharmacological Basis of Therapeutics (10th Edition) (Hardman et al., 2001).

Figure 2. The “free [I] with HMM $K_{i,app}$ ” method: comparison of predicted versus observed DDIs. The solid line depicts the line of unity; the long dashed line represents a two-fold deviation from unity; the short dashed line represents a three-fold deviation from unity (17 drugs and 59 clinical DDIs). The grids highlight four areas which represent the correct predictions for strong (observed AUC > 5, predicted AUC > 5), moderate ($2 \leq$ observed AUC \leq 5, $2 \leq$ predicted AUC \leq 5), weak interaction ($1.25 \leq$ observed AUC < 2, $1.25 \leq$ predicted AUC < 2) and no interaction (observed AUC < 1.25, predicted AUC < 1.25).

Figure 3. The “total [I] with plasma $K_{i,app}$ ” method: comparison of predicted versus observed DDIs. The solid line depicts the line of unity; the long dashed line represents a two-fold deviation from unity; the short dashed line represents a three-fold deviation from unity (17 drugs and 59 clinical DDIs). The grids highlight four areas which represent the correct predictions for strong (observed AUC > 5, predicted AUC > 5), moderate ($2 \leq$ observed AUC \leq 5, $2 \leq$ predicted AUC \leq 5), weak interaction ($1.25 \leq$ observed AUC < 2, $1.25 \leq$ predicted AUC < 2) and no interaction (observed AUC < 1.25, predicted AUC < 1.25).

Table 1. Kinetic parameters for CYP3A, CYP2C9 and CYP2D6 substrates from human hepatocyte suspensions in HMM or human plasma

<i>Substrate Parameters</i>	<i>HMM</i>	<i>Plasma</i>	<i>Unbound plasma</i>
Midazolam K_m (μM) [*]	8.11 \pm 0.65	45.83 \pm 4.38	1.47 \pm 0.14
Midazolam V_{max} (nmol/min/ million cells) [*]	0.021 \pm 0.001	0.036 \pm 0.001	-
Diclofenac K_m (μM) [*]	34.58 \pm 2.14	1408 \pm 304	4.22 \pm 0.91
Diclofenac V_{max} (nmol/min/ million cells) [*]	0.41 \pm 0.01	0.49 \pm 0.03	-
(R)-bufuralol K_m (μM) [*]	12.22 \pm 1.42	54.83 \pm 7.38	10.42 \pm 1.40
(R)-bufuralol V_{max} (nmol/min/ million cells) [*]	0.059 \pm 0.002	0.048 \pm 0.002	-

Note: The values of $f_{u,p}$ for midazolam, diclofenac and (R)-bufuralol were 0.032, 0.003 and 0.19.

^{*}Two systems (nominal values) showed the significant difference by T-test, $p < 0.05$.

Table 2. IC₅₀ values for CYP3A, CYP2C9 and CYP2D6 inhibitors from human hepatocyte suspensions in HMM and human plasma. Both HMM and plasma IC₅₀ values represented the nominal values obtained from each system.

<i>Inhibitor</i>	<i>IC₅₀ (μM)</i>		<i>f_{u,p}</i>
	<i>HMM IC₅₀</i>	<i>Plasma IC₅₀</i>	
<i>CYP3A Inhibitors</i>			
Ketoconazole	0.28 ± 0.02	1.26 ± 0.23 ^a	0.01
Fluconazole	27.00 ± 1.50	7.61 ± 2.67 ^a	0.89
Voriconazole	22.40 ± 4.90	3.01 ± 0.58 ^a	0.42
Conivaptan	1.90 ± 0.18	1.70 ± 0.56 ^a	0.01
Nefazodone	0.49 ± 0.08	1.70 ± 0.31 ^a	0.01
Aprepitant	Poor solubility	24.10 ± 7.30 ^a	0.05
<i>CYP2C9 Inhibitors</i>			
Miconazole	2.12 ± 0.37	2.02 ± 0.37	0.1
Fluconazole	53.96 ± 2.95	14.34 ± 1.27	0.89
Sulfaphenazole	0.29 ± 0.06	9.49 ± 1.89	0.32
Fluvastatin	4.07 ± 1.84	6.78 ± 1.01	0.01
Ibuprofen	151.30 ± 29.25	> 1200	0.01
Tolbutamide	101.08 ± 22.70	> 1200	0.04
<i>CYP2D6 Inhibitors</i>			
Diphenhydramine	1.71 ± 0.19	30.54 ± 4.34	0.22
Sertraline	3.10 ± 0.34	13.97 ± 3.49	0.01
Quinidine	0.03 ± 0.01	0.02 ± 0.01	0.13
Paroxetine	0.03 ± 0.01	0.07 ± 0.02	0.05
Fluoxetine	0.04 ± 0.00	0.35 ± 0.09	0.06
Duloxetine	0.22 ± 0.04	0.67 ± 0.37	0.05

Note: Each number represents the mean and standard error of estimate of triplicates.

^aFrom Mao et al., 2011

Table 3. Predictions of clinical DDIs from *in vitro* inhibition parameters of CPY3A, CYP2C9 and CYP2D6 inhibitors (63 clinical DDIs)

<i>Inhibitor</i>	<i>Victim drug</i>	<i>[I]_{ave, total}</i> <i>(μM)</i>	<i>HMM</i> <i>$K_{i,app}$</i> <i>(μM)</i>	<i>Plasma</i> <i>$K_{i,app}$</i> <i>(μM)</i>	<i>Predicted</i> <i>fold-increase</i> <i>in AUC by</i> <i>“Free [I] with</i> <i>HMM $K_{i,app}$”</i>	<i>Predicted fold-</i> <i>increase in</i> <i>AUC by “Total</i> <i>[I] with</i> <i>Plasma $K_{i,app}$”</i>	<i>Observed</i> <i>fold-</i> <i>increase in</i> <i>AUC</i>	<i>Reference</i>
Ketoconazole	Midazolam	2.82	0.26	0.75	1.93	6.60	15.90	(Olkkola et al., 1994)
Ketoconazole	Midazolam	3.46	0.26	0.75	1.96	7.41	16.00	(Tsunoda et al., 1999)
Ketoconazole	Midazolam	4.76	0.26	0.75	2.04	8.89	6.47	(Eap et al., 2004)
Ketoconazole	Midazolam	1.88	0.26	0.75	1.86	5.21	7.72	(Lam et al., 2003)
Ketoconazole	Midazolam	2.82	0.26	0.75	1.65	5.66	9.51	(Chung et al., 2006)
Ketoconazole	Midazolam iv.	3.46	0.26	0.75	1.12	4.24	5.10	(Tsunoda et al., 1999)
Ketoconazole	Midazolam	1.87	0.26	0.75	1.47	4.09	6.45	(McCrea et al., 1999)
Fluconazole	Midazolam	21.55	25.23	4.56	2.66	6.84	3.51	(Olkkola et al., 1996)
Fluconazole	Midazolam	29.99	25.23	4.56	2.84	7.70	3.60	(Olkkola et al., 1996)
Fluconazole	Midazolam	5.6	25.23	4.56	1.60	2.78	2.16	(Kharasch et al., 2005)
Aprepitant	Midazolam	1.72	-	14.43	-	1.92	2.27	(Majumdar et al., 2003)
Aprepitant	Midazolam	2.22	-	14.43	-	1.97	3.30	(Majumdar et al., 2003)

Aprepitant	Midazolam	0.41	-	14.43	-	1.72	1.28	(Majumdar et al., 2003)
Aprepitant	Midazolam iv.	3.11	-	14.43	-	1.26	1.47	(Majumdar et al., 2007)
Voriconazole	Midazolam iv.	1.64	20.93	1.80	1.03	1.79	3.64	(Saari et al., 2006)
Voriconazole	Midazolam	1.46	20.93	1.80	1.64	2.74	9.85	(Saari et al., 2006)
Nefazodone	Midazolam	1.73	0.46	1.02	1.79	4.17	4.44	(Lam et al., 2003)
Conivaptan	Midazolam	1.57	1.78	1.02	1.57	3.58	3	(NDA 021697)
Conivaptan	Midazolam iv.	1.57	1.78	1.02	1.00	2.29	2	(NDA 021697)
Sulfaphenazole	Tolbutamide	160	0.25	8.55	4.90	4.16	5.28	(Veronese et al., 1990)
Sulfaphenazole	Tolbutamide	320	0.25	8.55	4.95	4.53	3.09	(Back et al., 1988)
Sulfaphenazole	Phenytoin	640	0.25	8.55	3.99	3.85	3.05	(Hansen et al., 1979)
Fluconazole	S-warfarin	46.5	47.33	12.92	1.68	3.13	2.84	(Black et al., 1996)
Fluconazole	Tolbutamide	11.68	47.33	12.92	1.17	1.61	2.09	(Lazar and Wilner, 1990)
Fluconazole	Phenytoin	24	47.33	12.92	1.30	1.95	1.75	(Blum et al., 1991)
Fluconazole	Phenytoin	46.5	47.33	12.92	1.54	2.42	1.33	(Touchette et al., 1992)
Fluconazole	Losartan	23.4	47.33	12.92	1.33	2.01	1.69	(Kazierad et al., 1997)

Fluconazole	Losartan	23.4	47.33	12.92	1.33	2.01	1.27	(Kaukonen et al., 1998)
Fluconazole	Fluvastatin	23.4	47.33	12.92	1.22	1.63	1.84	(Kantola et al., 2000)
Fluconazole	Glimepiride	23.4	47.33	12.92	1.41	2.58	2.38	(Niemi et al., 2001)
Miconazole	S-warfarin	0.27	1.86	1.82	1.01	1.13	4.72	(O'Reilly et al., 1992)
Fluvastatin	Diclofenac	1	3.57	6.11	1.00	1.12	1.07	(Andersson et al., 2004)
Ibuprofen	Diclofenac	114	132.72	1081	1.00	1.08	0.99	(Andersson et al., 2004)
Tolbutamide	Diclofenac	165	88.67	1081	1.05	1.11	0.93	(Andersson et al., 2004)
iphenhydramine	Metoprolol	0.26	1.46	21.21	1.03	1.01	1.61	(Hamelin et al., 2000)
iphenhydramine	Metoprolol	0.26	1.46	21.21	1.03	1.01	1.10	(Hamelin et al., 2000)
iphenhydramine	Metoprolol	0.26	1.46	21.21	1.03	1.01	1.92	(Sharma et al., 2005)
iphenhydramine	Metoprolol	0.26	1.46	21.21	1.03	1.01	0.82	(Sharma et al., 2005)
Sertraline	Desipramine	0.071	2.65	9.70	1.00	1.01	1.24	(Preskorn et al., 1994)
Sertraline	Desipramine	0.065	2.65	9.70	1.00	1.01	1.37	(Alderman et al., 1997)
Sertraline	Desipramine	0.2	2.65	9.70	1.00	1.02	1.74	(Zussman et al., 1995)
Sertraline	Desipramine	0.2	2.65	9.70	1.00	1.02	1.54	(Kurtz et al., 1997)
Sertraline	Imipramine	0.2	2.65	9.70	1.00	1.01	1.68	(Kurtz et al., 1997)

Sertraline	Desipramine	0.2	2.65	9.70	1.00	1.02	2.29	(Kurtz et al., 1997)
Paroxetine	Desipramine	0.14	0.03	0.05	1.23	2.87	4.64	(Brosen et al., 1993)
Paroxetine	Imipramine	0.14	0.03	0.05	1.11	1.52	1.74	(Albers et al., 1996)
Paroxetine	Desipramine	0.14	0.03	0.05	1.23	2.87	4.28	(Albers et al., 1996)
Paroxetine	Metoprolol	0.14	0.03	0.05	1.21	2.60	7.93	(Hemeryck et al., 2000)
Paroxetine	Metoprolol	0.14	0.03	0.05	1.21	2.60	5.08	(Hemeryck et al., 2000)
Paroxetine	Desipramine	0.14	0.03	0.05	1.23	2.87	5.21	(Alderman et al., 1997)
Paroxetine	Desipramine	0.017	0.03	0.05	1.03	1.29	1.36	(Alderman et al., 1997)
Paroxetine	Desipramine	0.14	0.03	0.05	1.23	2.87	4.8	(Laine et al., 2004)
Quinidine	Desipramine	0.451	0.03	0.01	2.56	6.83	7.5	(Brosen and Gram, 1989)
Quinidine	Imipramine	0.451	0.03	0.01	1.47	1.81	1.54	(Brosen and Gram, 1989)
Quinidine	Encainide	0.451	0.03	0.01	2.47	6.03	3.18	(Funck-Brentano et al., 1989b)
Quinidine	Encainide	0.41	0.03	0.01	2.37	5.94	11.4	(Turgeon et al., 1990)
Quinidine	Metoprolol	0.23	0.03	0.01	1.80	4.59	3.24	(Johnson and Burlew, 1996)
Quinidine	Mexiletine	0.45	0.03	0.01	1.51	1.91	1.32	(Turgeon et al., 1991)
Quinidine	Propafenone	0.34	0.03	0.01	1.91	3.70	2.7	(Funck-Brentano et al., 1989a)

Quinidine	Desipramine	4.6	0.03	0.01	6.38	8.15	3.14	(Ayesh et al., 1991)
Fluoxetine	Desipramine	0.57	0.03	0.24	1.88	2.63	2.25	(Bergstrom et al., 1992)
Fluoxetine	Desipramine	1.54	0.03	0.24	2.98	4.19	7.43	(Bergstrom et al., 1992)
Duloxetine	Desipramine	0.3	0.19	0.47	1.07	1.53	2.9	(Skinner et al., 2003)

Table 4. Performances of two predictive methods for individual and all CYPs (CYP3A, CYP2C9 and CYP2D6 inhibitors)

	CYP3A		CYP2C9		CYP2D6		All CYPs	
	<i>Free [I] with HMM</i> <i>K_{i,app}</i>	<i>Total [I] with Plasma</i> <i>K_{i,app}</i>	<i>Free [I] with HMM</i> <i>K_{i,app}</i>	<i>Total [I] with Plasma</i> <i>K_{i,app}</i>	<i>Free [I] with HMM</i> <i>K_{i,app}</i>	<i>Total [I] with Plasma</i> <i>K_{i,app}</i>	<i>Free [I] with HMM</i> <i>K_{i,app}</i>	<i>Total [I] with Plasma</i> <i>K_{i,app}</i>
2-fold of Observed	26% ^a (5/19)	84% (16/19)	93% (14/15)	93% (14/15)	62% (18/29)	90% (26/29)	59% ^d (37/63)	89% (56/63)
No Interaction	NA ^b	NA	100% (3/3)	100% (3/3)	100% (3/3)	100% (3/3)	100% ^e (6/6)	100% (6/6)
Weak Interaction	0% (0/2)	100% (2/2)	80% (4/5)	80% (4/5)	20% (2/10)	40% (4/10)	35% (6/17)	59% (10/17)
Moderate Interaction	22% ^c (2/9)	67% (6/9)	33% (2/6)	66% (4/6)	10% (1/10)	60% (6/10)	20% (5/25)	64% (16/25)
Strong Interaction	0% (0/8)	63% (5/8)	0% (0/1)	0% (0/1)	0% (0/6)	33% (2/6)	0% (0/15)	47% (7/15)
GMFE	-	-	-	-	-	-	0.51	0.86
RMSE	-	-	-	-	-	-	3.94	2.61

- 26% (5/19) means that there are total 19 clinical studies related to CYP3A inhibitors. This method was able to predict 5 out of 19 within 2-fold of observed data;
- NA: there is no “No Interaction” in 19 CYP3A clinical studies;
- 22% (2/9) means that there are 9 (out of total 19) CYP3A clinical studies as “Moderate Interaction”. Among these 9 studies, this method was able to predict 2 clinical studies as moderate interactions;
- 59% (37/63) means that there are total 63 clinical studies related to CYP3A, CYP2C9 and CYP2D6 inhibitors. This method was able to predict 37 out of 63 within 2-fold of observed data;
- 100% (6/6) means that there are 6 (out of total 63) CYP3A clinical studies as “No Interaction”. Among these 6 studies, this method was able to predict all clinical studies as no interactions

Figure 1

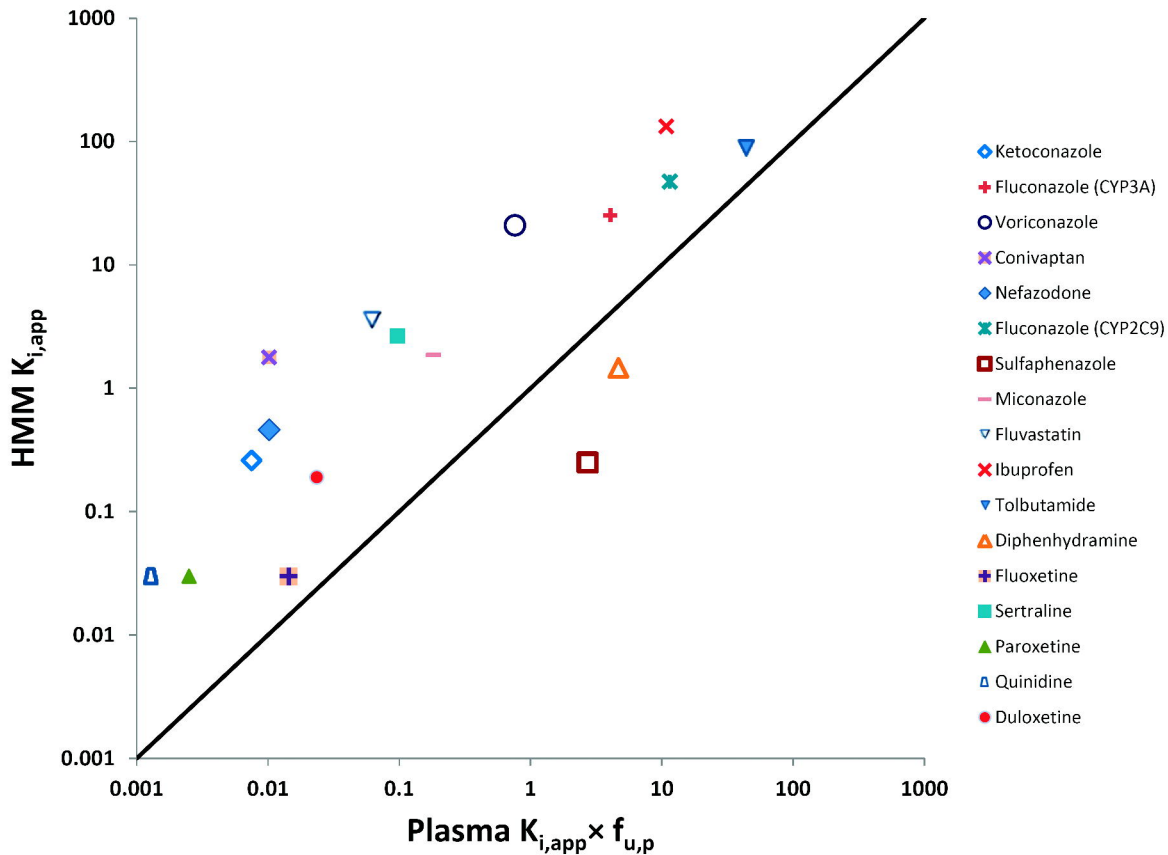


Figure 2

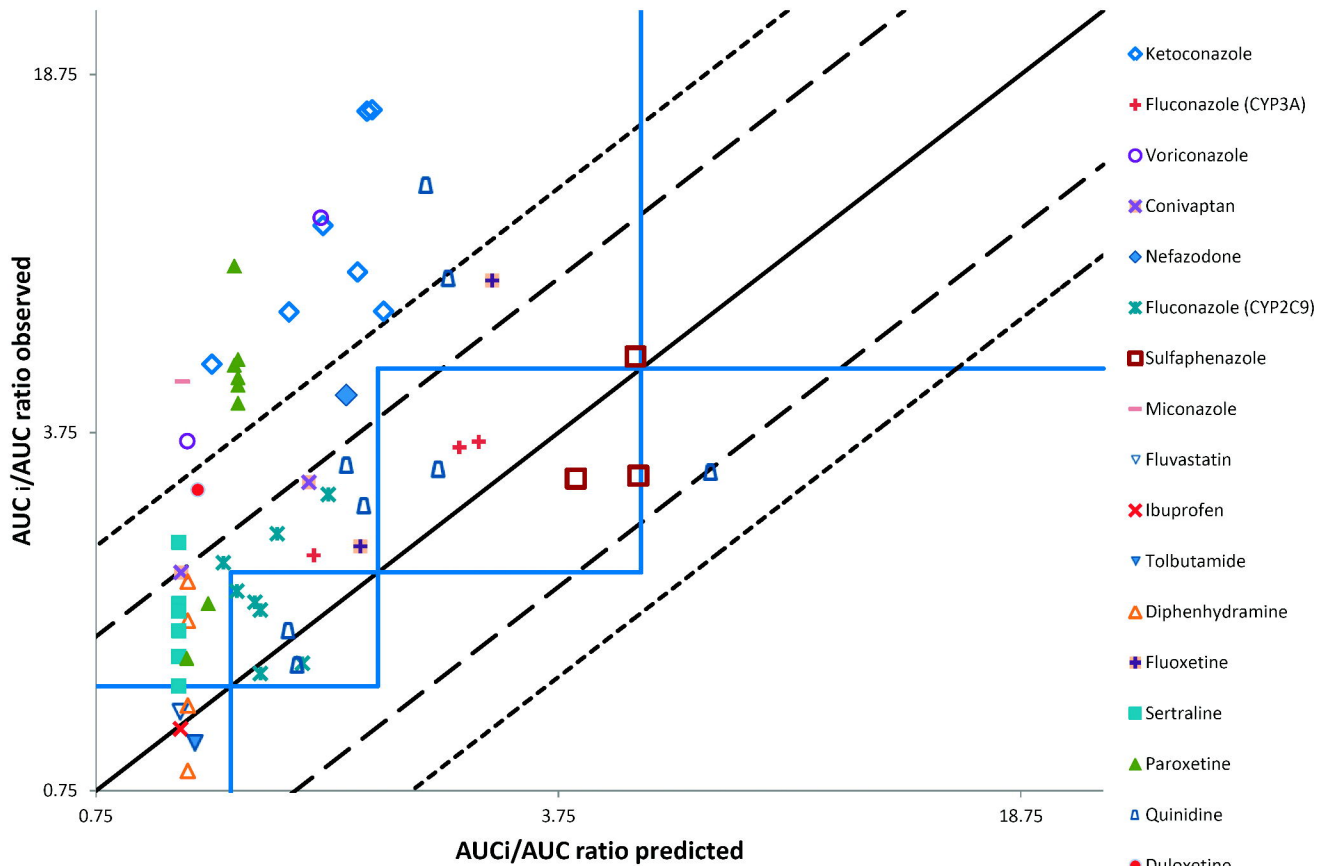


Figure 3

